Research Article | Vol. 24, No. 25 | 12 Dec 2016 | OPTICS EXPRESS 29001

Optics EXPRESS

Retrieval of ocean subsurface particulate backscattering coefficient from space-borne CALIOP lidar measurements

XIAOMEI LU,[1,2,*] YONGXIANG HU,[2,*] JACQUES PELON,[3] CHARLES TREPTE,[2] KATIE LIU,[4] SHARON RODIER,[1,2] SHAN ZENG,[1,2] PATRICIA LUCKER,[1,2] RON VERHAPPEN,[1,2] JAMIE WILSON,[1,2] CLAUDE AUDOUY,[5] CHRISTOPHE FERRIER,[6] SAID HAOUCHINE,[7] BILL HUNT,[1,2] AND BRIAN GETZEWICH[1,2]

[1]*Science Systems and Applications, Inc., 1 Enterprise Parkway, Suite, 200, Hampton, VA 23666, USA*
[2]*NASA Langley Research Center, Hampton, VA 23681, USA*
[3]*Centre National de la Recherche Scientifique (CNRS), Paris, France*
[4]*NIFS Internship at NASA Langley Research Center, Hampton, VA 23681, USA*
[5]*CALIPSO Mission Operations Manager CNES, Toulouse, France*
[6]*CALIPSO Flight Dynamics CNES, Toulouse, France*
[7]*CALIPSO Platform Engineer CNES, Toulouse, France*
[*]*xiaomei.lu@nasa.gov*

Abstract: A new approach has been proposed to determine ocean subsurface particulate backscattering coefficient b_{bp} from CALIOP 30° off-nadir lidar measurements. The new method also provides estimates of the particle volume scattering function at the 180° scattering angle. The CALIOP based layer-integrated lidar backscatter and particulate backscattering coefficients are compared with the results obtained from MODIS ocean color measurements. The comparison analysis shows that ocean subsurface lidar backscatter and particulate backscattering coefficient b_{bp} can be accurately obtained from CALIOP lidar measurements, thereby supporting the use of space-borne lidar measurements for ocean subsurface studies.

OCIS codes: (010.4458) Oceanic scattering; (010.3640) Lidar.

References and links

1. D. M. Winker, J. Pelon, J. A. Coakley, Jr., S. A. Ackerman, R. J. Charlson, P. R. Colarco, P. Flamant, Q. Fu, R. M. Hoff, C. Kittaka, T. L. Kubar, H. Le Treut, M. P. McCormick, G. Mégie, L. Poole, K. Powell, C. Trepte, M. A. Vaughan, and B. A. Wielicki, "The CALIPSO Mission: A Global 3D View of Aerosols and Clouds," Bull. Am. Meteorol. Soc. **91**(9), 1211–1229 (2010).
2. W. H. Hunt, D. M. Winker, M. A. Vaughan, K. A. Powell, P. L. Lucker, and C. Weimer, "CALIPSO Lidar description and performance assessment," J. Atmos. Ocean. Technol. **26**(7), 1214–1228 (2009).
3. M. A. Vaughan, S. A. Young, D. M. Winker, K. A. Powell, A. H. Omar, Z. Liu, Y. Hu, and C. A. Hostetler, "Fully automated analysis of space-based lidar data: an overview of the CALIPSO retrieval algorithms and data products," Proc. SPIE **5575**, 16–30 (2004).
4. M. J. Behrenfeld, Y. Hu, C. A. Hostetler, G. Dall'Olmo, S. D. Rodier, J. W. Hair, and C. Trepte, "Space-based lidar measurements of global ocean carbon stocks," Geophys. Res. Lett. **40**(16), 4355–4360 (2013).
5. M. J. Behrenfeld, Y. Hu, R. T. O'Malley, E. S. Boss, C. A. Hostetler, D. A. Siegel, J. Sarmiento, J. Schulien, J. W. Hair, X. Lu, S. Rodier, and A. J. Scarino, "Discovering Polar Phytoplankton Annual Cycles with a Space-Based Lidar," Nat. Geosci. submitted.
6. X. Lu, Y. Hu, C. Trepte, S. Zeng, and J. H. Churnside, "Ocean subsurface studies with the Calipso Spaceborne Lidar," J. Geophys. Res: Oceans **119**(7), 4305–4317 (2014).
7. J. Churnside, B. McCarty, and X. Lu, "Subsurface ocean signals from an orbiting polarization lidar," Remote Sens. **5**(7), 3457–3475 (2013).
8. Y. Hu, M. Behrenfeld, C. Hostetler, J. Pelon, C. Trepte, J. Hair, W. Slade, I. Cetinic, M. Vaughan, X. Lu, P. Zhai, C. Weimer, D. Winker, C. C. Verhappen, C. Butler, Z. Liu, B. Hunt, A. Omar, S. Rodier, A. Lifermann, D. Josset, W. Hou, D. MacDonnell, and R. Rhew, "Ocean lidar measurements of beam attenuation and a roadmap to accurate phytoplankton biomass estimates," EPJ Web of Conferences **119**, 22003 (2016).

#276046 http://dx.doi.org/10.1364/OE.24.029001
Journal © 2016 Received 21 Sep 2016; revised 1 Nov 2016; accepted 2 Nov 2016; published 7 Dec 2016

Optics EXPRESS

9. Y. Hu, K. Stamnes, M. Vaughan, J. Pelon, C. Weimer, D. Wu, M. Cisewski, W. Sun, P. Yang, B. Lin, A. Omar, D. Flittner, C. Hostetler, C. Trepte, D. Winker, G. Gibson, and M. Santa-Maria, "Sea surface wind speed estimation from space-based lidar measurements," Atmos. Chem. Phys. **8**(13), 3593–3601 (2008).
10. S. Rodier, P. Zhai, D. Josset, Y. Hu, and M. Vaughan, "Calipso lidar measurements for ocean subsurface studies," in *34th International Symposium on Remote Sensing of the Environment* (2011).
11. https://eosweb.larc.nasa.gov/HORDERBIN/HTML_Start.cgi
12. X. Lu, Y. Hu, C. Trepte, and Z. Liu, "A super-resolution laser altimetry concept," IEEE Geosci. Remote Sens. Lett. **11**(1), 298–302 (2014).
13. Y. Hu, K. Powell, M. Vaughan, C. Tepte, C. Weimer, M. Beherenfeld, S. Young, D. Winker, C. Hostetler, W. Hunt, R. Kuehn, D. Flittner, M. Cisewski, G. Gibson, B. Lin, and D. Macdonnell, "Elevation information in tail (EIT) technique for lidar altimetry," Opt. Express **15**(22), 14504–14515 (2007).
14. https://lta.cr.usgs.gov/GTOPO30
15. D. Josset, J. Pelon, and Y. Hu, "Multi-instrument calibration method based on a multiwavelength ocean surface model," IEEE Geosci. Remote Sens. Lett. **7**(1), 195–199 (2010).
16. X. Zhang, L. Hu, and M. X. He, "Scattering by pure seawater: effect of salinity," Opt. Express **17**(7), 5698–5710 (2009).
17. X. Zhang and L. Hu, "Estimating scattering of pure water from density fluctuation of the refractive index," Opt. Express **17**(3), 1671–1678 (2009).
18. A. Morel, D. Antoine, and B. Gentili, "Bidirectional reflectance of oceanic waters: accounting for Raman emission and varying particle scattering phase function," Appl. Opt. **41**(30), 6289–6306 (2002).
19. M. S. Twardowski, H. Claustre, S. A. Freeman, D. Stramski, and Y. Huot, "Optical backscattering properties of the "clearest" natural waters," Biogeosci. **4**(6), 1041–1058 (2007).
20. http://oceandata.sci.gsfc.nasa.gov/MODIS-Aqua/Mapped/Monthly/9km/Kd
21. NASA Goddard Space Flight Center, Ocean Ecology Laboratory, Ocean Biology Processing Group, "Moderate-Resolution Imaging Spectroradiometer (Modis) Aqua Downwelling Diffuse Attenuation Coefficient Data," 2014 Reprocessing. NASA OB.DAAC, Greenbelt, MD, USA.
22. C. D. Mobley, B. Gentili, H. R. Gordon, Z. Jin, G. W. Kattawar, A. Morel, P. Reinersman, K. Stamnes, and R. H. Stavn, "Comparison of numerical models for computing underwater light fields," Appl. Opt. **32**(36), 7484–7504 (1993).
23. J. M. Sullivan and M. S. Twardowski, "Angular shape of the oceanic particulate volume scattering function in the backward direction," Appl. Opt. **48**(35), 6811–6819 (2009).
24. A. L. Whitmire, W. S. Pegau, L. Karp-Boss, E. Boss, and T. J. Cowles, "Spectral backscattering properties of marine phytoplankton cultures," Opt. Express **18**(14), 15073–15093 (2010).
25. S. A. Garver and D. A. Siegel, "Inherent optical property inversion of ocean color spectra and its biogeochemical interpretation: 1. time series from the sargasso sea," J. Geophys. Res: Oceans **102**(C8), 18607–18625 (1997).
26. A. L. Whitmire, E. Boss, T. J. Cowles, and W. S. Pegau, "Spectral variability of the particulate backscattering ratio," Opt. Express **15**(11), 7019–7031 (2007).
27. http://oceancolor.gsfc.nasa.gov/cms/atbd/rrs
28. NASA Goddard Space Flight Center, Ocean Ecology Laboratory, Ocean Biology Processing Group, "Moderate-Resolution Imaging Spectroradiometer (Modis) Aqua Remote-Sensing Reflectance Data," 2014 Reprocessing. NASA OB.DAAC, Greenbelt, MD, USA.
29. Z. Lee, K. L. Carder, and R. A. Arnone, "Deriving inherent optical properties from water color: a multiband quasi-analytical algorithm for optically deep waters," Appl. Opt. **41**(27), 5755–5772 (2002).
30. http://oceandata.sci.gsfc.nasa.gov/MODIS-Aqua/Mapped/Monthly/9km/
31. M. Chami, D. McKee, E. Leymarie, and G. Khomenko, "Influence of the angular shape of the volume-scattering function and multiple scattering on remote sensing reflectance," Appl. Opt. **45**(36), 9210–9220 (2006).
32. Z. Lee, K. Du, and R. Arnone, "A model for the diffuse attenuation coefficient of downwelling irradiance," J. Geophys. Res: Oceans **110**(C2), 1–10 (2005).

1. Introduction

The Cloud-Aerosol Lidar with Orthogonal Polarization (CALIOP), a space-borne two-wavelength (532 nm and 1064 nm) and polarization-sensitive lidar (with cross-polarized and co-polarized channels at 532 nm), is the primary payload instrument on the Cloud-Aerosol Lidar and Infrared Pathfinder Satellite Observations (CALIPSO) satellite. The CALIOP lidar was designed to provide the observations necessary for an improved understanding of the impact of clouds and aerosols on the Earth's radiation budget and climate [1–3]. Current analyses indicate a potential of CALIOP lidar for quantifying global ocean carbon stocks [4, 5] and ocean subsurface backscatter [6–8] as well.

For the CALIOP near nadir (0.3° or 3° off nadir angles) measurements, the ocean surface attenuated backscatter is about 30 times stronger than the subsurface backscatter [8, 9], which makes it difficult to separate the subsurface backscatter from ocean surface backscatter [6, 10]. Behrenfeld et al. quantified the global ocean phytoplankton biomass and total particulate

organic carbon stocks using CALIOP near nadir measurements, where the ocean surface backscatter was estimated from co-located Advanced Microwave Scanning Radiometer-EOS (AMSR-E) ocean surface wind speed and CloudSat microwave measurements, and particulate depolarization ratio in water was evaluated using MODerate-resolution Imaging Spectroradiometer (MODIS) monthly diffuse attenuation coefficients [4]. Lu et al. estimated the profile of ocean subsurface backscatter by a de-convolution process to remove the contamination by the surface backscatter [6]. Churnside et al. [7] showed evidence of ocean subsurface backscatter based on the delay and broadening of the cross-polarized signal relative to the co-polarized signal in the three near-surface range bins.

However, if the lidar is pointed 30° off nadir, the ocean surface signal is reduced by more than two orders of magnitude and CALIOP lidar can then accurately measure ocean subsurface backscatter. The objective of this study is to estimate the ocean subsurface lidar backscatter and particulate backscattering coefficient b_{bp} from CALIOP 30° off nadir observations. This study also provides a way to calculate the volume scattering function (VSF) at the 180° scattering angle, which is difficult to measure in practice due to the complex design of instrument especially at far backward angle near 180°.

2. Method

The ocean layer-integrated attenuated backscatter (unit: sr^{-1}) is defined as:

$$\gamma_\lambda = \int_{surface-300m}^{surface+30m} \beta'_\lambda(z)dz \tag{1}$$

where β'_λ (unit: km^{-1} sr^{-1}) is the total attenuated backscatter at λ = 532 nm or 1064 nm from CALIOP level 1 data products which are available to public [11]. Because the CALIOP lidar receiver's transient response affects the magnitude of the attenuated backscatter vertical distribution [12, 13], the integration in Eq. (1) is between 30 meters above and 300 meters below the surface, where the surface is determined to be the maximum attenuated backscatter located within 150 meters above or below the reported Global 30 Arc-Second (GTOPO30) Digital Elevation Model (DEM) [14]. This procedure allows for small variations in GTOPO30 DEM accuracy and eliminates most of the dense, low-lying atmospheric layers that could be mistaken as surface echo. The ocean subsurface layer-integrated backscatter (unit: sr^{-1}) at 532 nm is finally estimated as:

$$\gamma_t = \frac{\gamma_{532} - 0.7\gamma_{1064}}{T_{532}^2} \tag{2}$$

where γ_{532} is the two-way atmospheric transmittance at 532 nm derived from meteorological data reported in the CALIOP level 1 files. For this study, we only analyze cases under clear sky conditions so that the γ_{532} term provides an accurate estimate of the total signal attenuation between the lidar and the Earth's surface. In this paper, clear sky cases are defined as single laser shot measurements having the integrated attenuated backscatter (IAB) at 532nm of the column above the surface lower than 0.017/sr [15]. The use of IAB <0.017/sr warrants the air column is sufficiently clear and clean. The second term in the numerator of Eq. (2) stands for the surface contribution to the 532 nm subsurface backscatter, which was estimated using 1064 nm observations as its subsurface signals are near zero due to strong absorption by water at 1064 nm. Observations suggest that ocean surface backscatter at 532 nm is about 30% less than ocean surface backscatter at 1064 nm due to more atmospheric attenuation and ozone absorption at 532 nm [8].

Optics EXPRESS

The ocean subsurface particulate backscatter is $\gamma_p = \gamma_t - \gamma_w$, where γ_w is the water molecules integrated lidar backscatter and can be estimated as $\gamma_w = \frac{1.6\times10^{-4}}{2K_d}$ (sr^{-1}) [7, 16–19], with the diffuse attenuation coefficient (K_d) from MODIS Aqua ocean color measurements [20, 21]. Here we used the ocean level 3 monthly K_d products at 490 nm scaled to 532 nm, $K_{d,532} = 0.68(K_{d,490} - 0.022) + 0.054$, because there are not enough daily K_d measurements co-located with CALIOP lidar 30° off nadir measurements under clear sky conditions. With the value of ocean subsurface particulate backscatter γ_p, the particulate volume scattering function (VSF) at the 180° scattering angle $\beta_p(\pi)$ (unit: sr^{-1} m^{-1}) can be estimated as [4, 22]:

$$\beta_p(\pi) = \frac{2m^2 K_d \gamma_p}{t^2} \tag{3}$$

where t is the ocean surface transmittance (~0.98 at 532 nm) and m is refractive index of water (~1.32 at 532 nm). Retrieved values of $\beta_p(\pi)$ from Eq. (3) are then related to the hemispheric backscattering coefficient b_{bp} (unit: m^{-1}) using a mean particulate phase function in the backward direction $\beta_p(\pi)/b_{bp}$ value of 0.16 sr^{-1} [23, 24]. The particulate backscattering coefficient b_{bp} at 443 nm is finally calculated as:

$$b_{bp} = \frac{\beta_p(\pi)}{0.16}\frac{532}{443} = \frac{2m^2 K_d \gamma_p}{0.16t^2}\frac{532}{443} \tag{4}$$

where the final factor 532/443 in Eq. (4) relates b_{bp} at 532 nm to b_{bp} at 443 nm assuming a spectral slope of −1 for particulate backscattering coefficient [25, 26]. Collectively, Eq. (2), (3) and (4) provide the link between space-born lidar measurements and passive ocean color imagery, which will be shown in the next section. Compared with the methods using co-located AMSR-E wind speed to estimate the ocean surface backscatter [4, 6, 9, 10], the advantage of the new method is that the ocean surface contribution at 532 nm is estimated directly from CALIOP 1064 nm observations and values of particulate depolarization ratio in water and CALIOP's receiver transient response are not required. Moreover, Eq. (3) provides a way to calculate the Volume Scatter Function (VSF) at the 180° scattering angle $\beta_p(\pi)$. In practice, it is difficult to measure the full VSF (0°-180°) due to two reasons, one is the complex design of instrumentation required to make a large number of discrete measurements over a broad angular range especially at the near forward 0° and far backward 180° scattering angles, and the other one is the large dynamic range in signal (typically greater than 4 orders of magnitude) that must be resolved [23].

3. Results

The CALIOP lidar was tilted 30° off-nadir in order to minimize ocean surface backscatter and demonstrate the lidar ocean subsurface measurement concept from space [8]. The red, pink, green, yellow and black lines in Fig. 1 show the CALIOP footprints of 30° off-nadir measurements on July 17 2014, September 23 2015, October 7 2015, October 21 2015 and April 13 2016, respectively. The background color is the MODIS monthly diffuse attenuation coefficient K_d at 532 nm in July 2014. The observed lidar attenuated backscatter profiles for the lowest 1 km on July 17 2014 are shown in Fig. 2, which indicates that ocean subsurface backscatter can be clearly detected from both 532 nm parallel (upper panel) and perpendicular (middle panel) channels (red circles), while very little ocean surface backscatter is seen at 1064 nm channel (lower panel red circle).

Optics EXPRESS

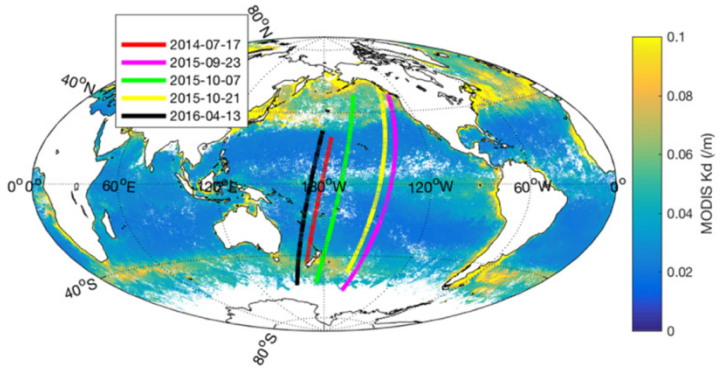

Fig. 1. Orbit tracks when CALIOP lidar is tilted 30° off-nadir on different dates. The background color is the MODIS diffuse attenuation coefficient (K_d) map scaled to 532 nm.

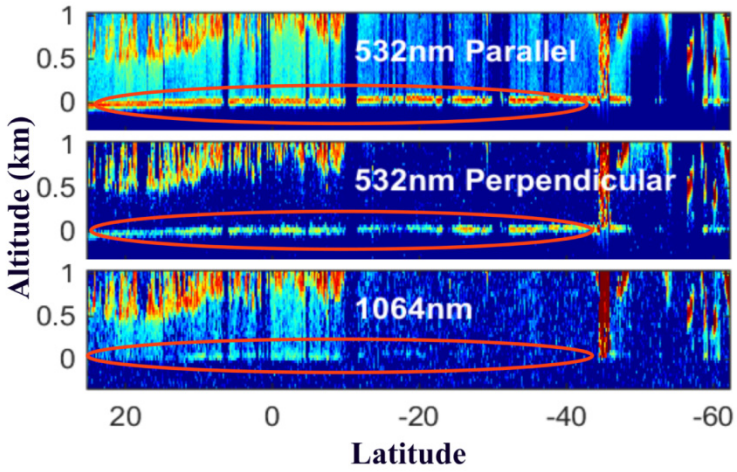

Fig. 2. The lowest 1 km CALIOP backscatter profiles on July 17 2014. Upper panel: 532 nm parallel channel; middle panel: 532nm perpendicular channel; lower panel: 1064 nm channel [8].

The CALIOP retrieved results on July 17 2014 are shown in Fig. 3 with the upper panel giving the CALIOP retrieved ocean subsurface layer-integrated backscatter γ_t (sr^{-1}) at 532 nm (blue dots) from Eq. (2) and co-located MODIS remote sensing reflectance (R_{rs}) at 531 nm (red dots). MODIS remote sensing reflectance is the fundamental quantity to be derived from ocean color sensors because it provides the basic input to many derived product algorithms [27, 28]. The CALIOP retrieved particulate backscattering coefficient b_{bp} (blue dots) from Eq. (4) is compared with MODIS b_{bp} at 443 nm (red line shown in Fig. 3(b)) which was retrieved from quasi-analytical algorithm [29]. The MODIS level 3 monthly K_d, R_{rs} and b_{bp} products are used here and can be downloaded from the NASA's Ocean Color website [30]. Lower panel of Fig. 3 gives the particulate VSF at the 180° scattering angle $\beta_p(\pi)$ from Eq. (3). The $\beta_p(\pi)$ values range from 1×10^{-3} sr^{-1} m^{-1} to 1×10^{-4} sr^{-1} m^{-1} at the CALIOP lidar measured locations with latitude changing from 45°S to 30°N. These CALIOP retrieved $\beta_p(\pi)$ values in oceanic water are comparable to previous recorded particulate VSFs (e.g. 10^{-4} ~10^{-2} sr^{-1} m^{-1}) [23, 31]. Figure 4 is CALIOP retrieved ocean subsurface backscatter γ_t (blue dots) with co-located MODIS R_{rs} results (red dots) on different 30° off-nadir measurement dates. Figure 5 is the corresponding particulate backscattering coefficient b_{bp} comparison between CALIOP retrieved results (blue dots) and MODIS results (red dots).

Optics EXPRESS

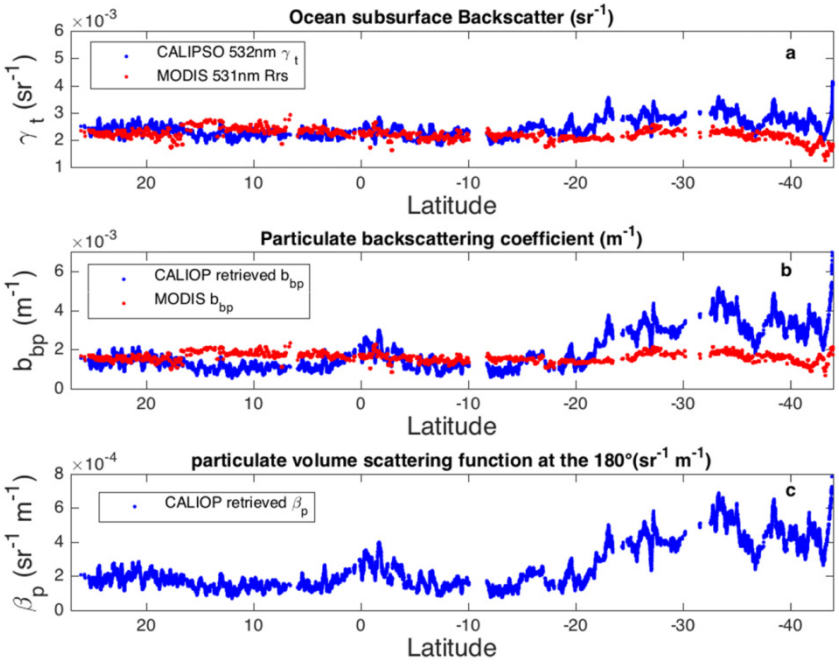

Fig. 3. Upper panel: CALIOP retrieved ocean subsurface backscatter at 532 nm (blue dots) on July 17 2014 was compared with co-located MODIS remote sensing reflectance R_{rs} at 531 nm (red dots). Middle panel: CALIOP retrieved particulate backscattering coefficient b_{bp} (blue dots) on July 17 2014 with co-located MODIS b_{bp} at 443 nm (red dots). Lower panel: CALIOP retrieved particulate VSF at the 180° scattering angle on July 17 2014.

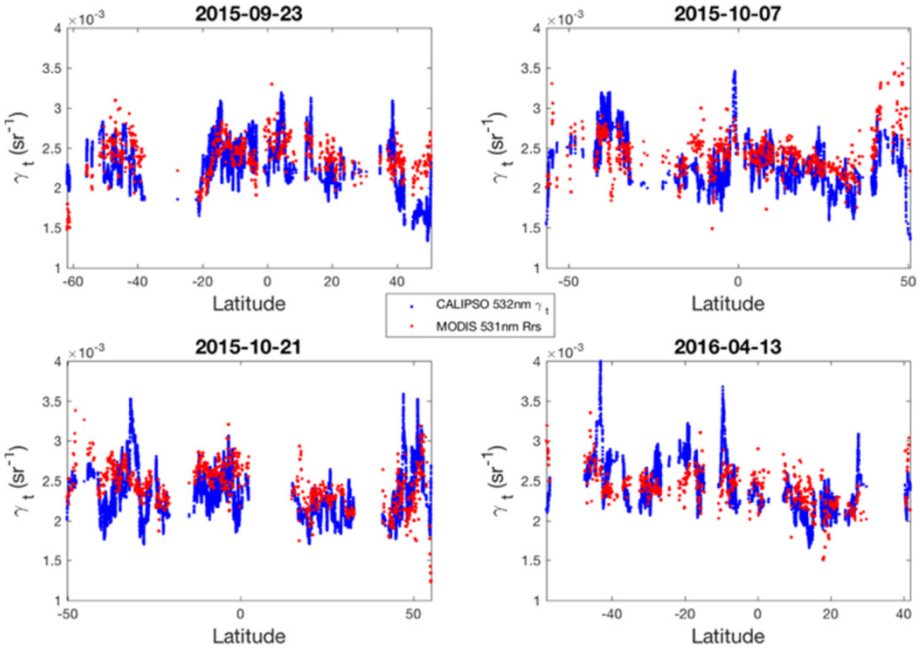

Fig. 4. CALIOP retrieved ocean subsurface integrated backscatter γ_t at 532 nm (blue dots) with co-located MODIS R_{rs} results at 531 nm (red dots) on different measurement dates.

Optics EXPRESS

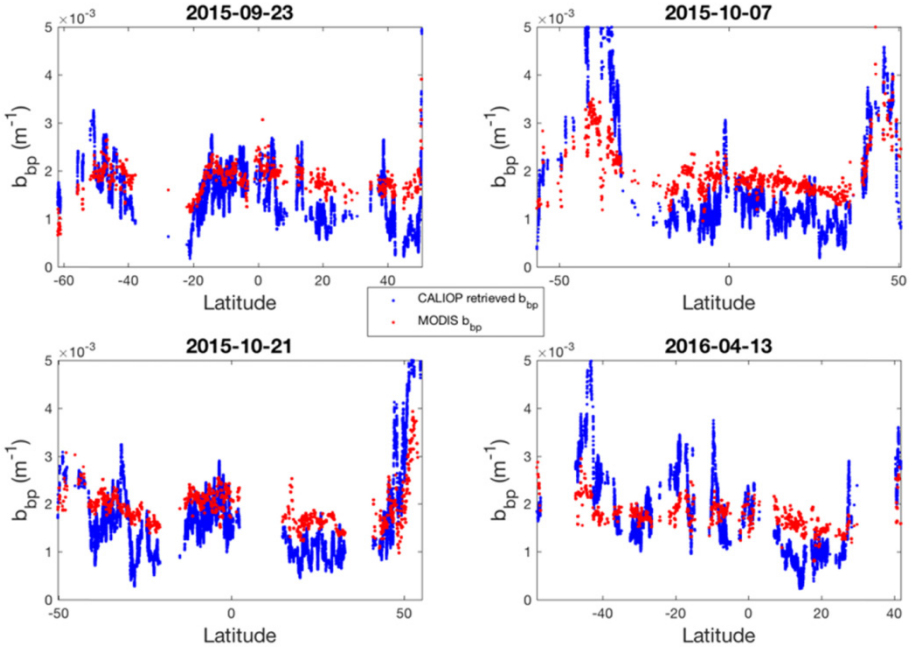

Fig. 5. CALIOP retrieved particulate backscattering coefficient b_{bp} at 443 nm (blue dots) with co-located MODIS b_{bp} results (red dots) on different measurement dates.

As shown in Fig. 3, the CALIOP retrieved ocean subsurface layer-integrated backscatter γ_t (sr^{-1}) at 532 nm compares reasonably well with MODIS R_{rs} at 531 nm. The mean relative difference between CALIOP γ_t and MODIS R_{rs} ($\frac{\gamma_t - R_{rs}}{R_{rs}} \times 100\%$) is about 13%, which is mainly due to the time offset and different measurement sites. CALIOP lidar observations were acquired on July 17, 2014 while MODIS R_{rs} was from monthly products of July 2014, and the distance between CALIOP and MODIS footprints can be as high as 13 km. The root mean square of difference between CALIOP γ_t and MODIS R_{rs} is about 5.4×10^{-4} sr^{-1}. The error contribution from uncertainty of factor 0.7 in Eq. (2) is negligible because at 30° off nadir the ocean surface backscatter at 1064 nm is small compared to the subsurface backscatter at 532 nm as results shown in Fig. 2. For example, the mean relative difference of γ_t is about 0.89% with root mean square error of 3.5×10^{-5} sr^{-1} when the factor of 0.7 in Eq. (2) has 15% uncertainty. For the cases shown in Fig. 4, the mean relative differences between CALIOP γ_t and MODIS R_{rs} at each day are less than 10% with root mean square less than 3.5×10^{-4} sr^{-1}. Source of uncertainty of CALIOP retrieved b_{bp} from Eq. (4) include measurement errors and errors associated with assumptions regarding particulate scattering optical properties, such as ratio of $\beta_p(\pi)/b_{bp}$ value of 0.16 sr^{-1}, and wavelength dependence of b_{bp}. From Eq. (4), the uncertainty of particulate backscattering coefficient can be estimated as:

$$\frac{\Delta^2 b_{bp}}{b_{bp}^2} = \frac{\Delta^2 \frac{\beta_p(\pi)}{b_{bp}}}{(\frac{\beta_p(\pi)}{b_{bp}})^2} + \frac{\Delta^2 \frac{b_{bp,443}}{b_{bp,532}}}{(\frac{b_{bp,443}}{b_{bp,532}})^2} + \frac{\Delta^2 K_d}{K_d^2} + \frac{\Delta^2 \gamma_p}{\gamma_p^2} \quad (5)$$

Here, the ratio of $\beta_p(\pi)/b_{bp}$ value is assumed to be 0.16 sr^{-1} with 10% uncertainty [23, 24]. We assume a 10% uncertainty for both the diffuse attenuation coefficient K_d [32] and the wavelength dependence of b_{bp} [25]. Uncertainty of ocean subsurface particulate backscatter γ_p

Optics EXPRESS

is estimated as 20% due to contributions from both CALIOP retrieved γ_t and water molecules lidar backscatter γ_w. Summing up all the uncertainties yields the value of Eq. (5) as 0.07, resulting the uncertainty in the CALIOP retrieved b_{bp} is about 26%. This is in agreement with b_{bp} results shown in Fig. 3(b) and 5, where most of the mean relative difference for each day are less than 20% with a maximum of about 29%. The root mean square of difference between CALIOP and MODIS b_{bp} are less than 1.5×10^{-3} m^{-1}. Compared to the errors analyzed above, the contributions due to the uncertainties of ocean surface transmittance and refractive index of water are negligible and not considered in Eq. (5).

4. Conclusion

Within this study, we introduce an approach for estimating the ocean subsurface layer-integrated backscatter γ_t (sr^{-1}) and particulate backscattering coefficient b_{bp} (m^{-1}) from CALIOP 30° off-nadir lidar measurements. The approach also provides a way to calculate the particulate volume scattering function at the 180° scattering angle that is difficult to measure in practice. The advantage of this method is that ocean surface backscatter at 532 nm is estimated directly from 1064 nm observations as ocean subsurface signals are near zero at 1064 nm due to the strong water absorption at this wavelength. The CALIOP retrieved γ_t (sr^{-1}) and b_{bp} (m^{-1}) compare favorably with results from MODIS ocean color data. The CALIOP retrieved ocean subsurface results can help understand the different optical properties of various water masses and quantify global ocean carbon stocks and ocean phytoplankton biomass. Our findings support the use of space-borne lidar measurements, such as CALIOP lidar for ocean subsurface studies.

5. Acknowledgments

MODerate-resolution Imaging Spectroradiometer (MODIS) Aqua downwelling diffuse attenuation coefficient k_d data, remote-sensing reflectance R_{rs} data and particulate backscattering coefficient b_{bp} data are provided by the NASA Ocean Color Data Web (http://oceandata.sci.gsfc.nasa.gov accessed on 08/11/2016).